

# Research Journal of Pharmaceutical, Biological and Chemical Sciences

## The Effect of Operation Conditions and Physical Characteristics of The Suspension-Carrying Flow in A Vertical Pipeline on The Near-Wall Transverse Migration of Solid Particles.

Albert Konstantinovich Papovyants\*, Valery Petrovich Mel'nikov,  
Igor Alekseevich Voronin, and Vitaly Vladimirovich Grigorov.

Joint Stock Company – State Scientific Centre of the Russian Federation – Institute for Physics and Power Engineering named after A.I. Leypunsky (JSC “SSC RF –IPPE”) Russia, 249033 Kaluga region, Obninsk, Bondarenko, 1.

### ABSTRACT

The objective of the work is to analyze the behavior of suspended solid particles in the vertical flow of the carrying medium (liquid, gas) and to identify thermo-hydraulic and other factors that impact the transverse migration of these particles in the laminar sublayer. It has been shown that a significant near-wall liquid velocity gradient can result in occurrence of a transverse lift force (Saffman force) affecting the particle. In this case, the particle migration to the wall and from the wall depends on the particle size, particle-to-flow density ratio,  $\rho_p / \rho_f$ , hydrodynamic mode (Reynolds number) and flow direction (downwards or upwards). It has been demonstrated that in the upward vertical flow, at  $\rho_p / \rho_f < 1$ , the particle is impacted by the transverse force in the direction to the wall. In the same flow but at  $\rho_p / \rho_f > 1$ , the transverse force acts in the direction from the wall. Thus, in case of the downward vertical flow, the effect for each indicated density ratio changes into the opposite one. In compliance with the equations of particle motion in the turbulent liquid or gas flows, the required computer calculations were made for the eutectic alloy Pb-Bi ( $\rho_p < \rho_f$ ), lithium Li ( $\rho_p > \rho_f$ ) and air ( $\rho_p \gg \rho_f$ ), at their flow in the circular tubes of various diameter and in different modes. The equation was derived for the time-constant transverse component of the particle velocity in the laminar sublayer. The calculation results have been qualitatively confirmed by the experiment performed for the tubes with both upward and downward flows of Pb-Bi coolant that contained solid particles of a wide range of sizes. The obtained data testify to the presence of a transverse lift force affecting the particles in the laminar sublayer of the flow in the vertical channel. This effect should be taken into account, in particular, in prediction of deposits formation on the channel walls of various process equipment.

**Keywords:** laminar sublayer, particle, transverse migration, Saffman force, vertical pipe, calculation, experiment, lead-bismuth, lithium.

*\*Corresponding author*

## INTRODUCTION

The research into wall flows of liquid and gas media that contain dispersed particles is topical for a wide group of technical applications. It covers hydrodynamic and aerodynamic processes of suspension-carrying flows in industrial systems of various application (nuclear reactor core channels, mining equipment used to transport liquid materials, such as uranium- or gold-bearing materials), as well as in aircrafts in dusty atmosphere, rocket engine nozzles in two-phase working medium, etc[1-4].

In the above-mentioned examples, a significant role can be played by a shear boundary layer present close to the streamlined surface due to carrying flow viscosity under the influence of the transverse (as regard to the main flow) Saffman lift force[5-8] that affects the particles. This force results in certain changes in dispersed phase spatial distribution, which, in its turn, results, in particular, in particles separation with the following possible formation of deposits on the channel walls, annular concentration of particles in the flow, etc.

It should be stressed that hydrodynamics of near-wall suspension layers is much less studied as compared to the issues of aeromechanics of dusty atmosphere near-wall layers [9-14]. In contrast to gas, in shear flows of dropping liquids a typical transverse migration of low-inertia particles is a slow process caused by weak forces that depend on the distance to the channel wall, velocity profile and presence of other particles. In literature there are still very few publications dedicated to analytical and experimental studies of laminar shear flows of media with moderately different inertial phase properties [15-16], such as liquid coolants and other suspension-carrying flows. Sophistication and complexity of experimental techniques and the necessity to use expensive equipment facilitates the development of mathematical models aimed without limitation at identification of conditions for transverse migration of weakly inertial particles to occur in shear flows.

## MATERIALS AND RESEARCH METHODS

Let us consider a steady turbulent liquid flow, which contains suspended particles, in a vertical circular pipe with a diameter equal to  $d$ . The concentration of particles is such that it does not affect the liquid velocity profile. The particles entrained into eddies diffuse within the turbulent core in the way similar to that of the carrying liquid. Under the influence of viscous forces, the particles move in accordance with the velocity distribution that exists in the flow. The concentration profile of suspended particles in the turbulent core, likewise that of the dissolved impurities, is close to the flat one. The particles have a spherical shape and their size is so small that the resistance resulting from their relative motion is described by the Stokes' law. Physical and chemical phenomena in the laminar sublayer of the liquid are not considered.

Near the wall a particle starts to interact with a shear liquid flow, and its following behavior will depend on the result of this interaction: it may continue its motion towards the wall or it may be pushed away to the center of the flow.

If it is assumed that within part of the buffer (as quasi-laminar) layer and within the laminar sublayer of the carrying flow the only force that acts on the particle in the course of its motion towards the wall is the Stokes' drag force, the particle motion equation for the radial component will be the following:

$$-6\pi\mu \cdot \sigma v_p = \frac{4}{3} \pi \sigma^3 \rho_p \frac{dv_p}{d\tau} , \quad (1)$$

Where  $v_p$  is a radial component of the particle velocity,  $\mu$  is a liquid dynamic viscosity,  $\sigma$  is a particle radius,  $\rho_p$  is a particle density,  $\tau$  stands for time.

After a simple rearrangement of equation (1) and its integration from the initial moment  $\tau = 0$  of the particle motion, when its velocity is  $v_p^0$ , to the time  $\tau$ , we will get:

$$v_p = v_p^0 \exp\left(-4.5 \frac{\mu}{\rho_p \sigma^2} \tau\right) = v_p^0 \exp(-\beta \tau) \tag{2}$$

Let us perform estimate calculations of  $v_p$  as applied, for example, to the model liquid, i.e. lead-bismuth eutectics (55,5 % Bi, 44,5 Pb %) chosen due to its use for further experimental confirmation of the calculated results, with the following conditions and parameters:  $t = 300^\circ\text{C}$ ;  $\mu = 20 \cdot 10^{-4} \text{ kg/ms}$ ;  $\rho_p = 7.8 \cdot 10^3 \text{ kg/m}^3$ ;  $\sigma = 5.0 \text{ }\mu\text{m}$ . Then:

$$\beta = 4.5 \frac{20 \cdot 10^{-4}}{7.8 \cdot 10^3 \cdot (5.0 \cdot 10^{-6})^2} = 4.6 \cdot 10^4, 1/s$$

And thus, during the time of the particle motion equal, for instance, to  $\tau \approx 1 \cdot 10^{-3}\text{s}$ , its radial velocity will be:

$$v_p = v_p^0 \exp(-4.6 \cdot 10^4 \cdot 1 \cdot 10^{-3}) \sim 1.0 \cdot 10^{-20} v_p^0$$

Thus, it follows that even during the chosen short period of time of its motion the particle is slowed down from the initial velocity  $v_p^0$  actually to its zero value. Consequently, the distance  $S_c$  covered by the particle under the inertial force with account of Stokes' drag force is also negligibly short:

$$S_c = \int_0^\infty v_p^0 \exp(-\beta \tau) d\tau = \frac{1}{\beta} v_p^0 = \frac{1}{4.6 \cdot 10^4} = 1.25 \cdot 10^{-4} v_p^0. \tag{3}$$

So, in case of only inertial motion of a dense particle in the laminar layer and in part of buffer layer, under the influence of only one force, i.e. the Stokes' drag force, the very fact of its reaching the wall in the liquid flow is ruled out.

Under the viscous conditions of a particle motion through the stagnated liquid, in the absence of external forces, the Stokes' drag force is actually the only force acting on it. However, in the turbulent flow neither laminar, nor buffer layers are stagnated; on the contrary, they are characterized by a high velocity gradients. Systematic occurrence of transverse lift force is shown in Figure 1. In the case under consideration, the dense particle motion towards the wall of the vertical pipe with a diameter of  $d$  is provided under condition when its initial axial velocity is sufficient for the difference between local velocities of the particle and the flow  $U_p - U_f$  in the near-wall layer to be higher than zero. Otherwise, the direction of the particle motion changes to the opposite.

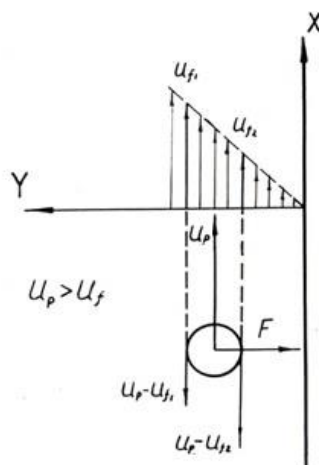


Figure 1 – Occurrence of transverse Saffman lift force for a particle in the wall liquid flow.

In further calculations, in order to study the influence of this effect on particle motion in the dropping liquid let us use the analytical equation for Saffman lift force  $F$  [3] derived for unlimited shear flow:

$$F = k\sigma^2(U_p - U_f) \sqrt{\mu\rho_f \left| \frac{dU_f}{dy} \right|}, \tag{4}$$

where  $U_p-U_f$  is a particle slip velocity;  $\rho_f$  – flow density;  $k = 6.46$  is a constant derived from numerical integral evaluation.

(Hereinafter, indices "f" and "p" refer respectively to flow and particle; the other symbols remain the same). To use equation (4), it is sufficient to meet three conditions indicated in [3], namely:

$$Re_k = \frac{\sigma^2}{\nu} \frac{dU_f}{dy} \ll 1; \quad Re_{U_p-U_f} = \frac{(U_p - U_f)\sigma}{\nu} \ll Re_k^{1/2}; \quad Re_\omega = \frac{\omega\sigma^2}{\nu} \ll 1. \tag{5}$$

Here  $\nu$  is flow kinematic viscosity,  $\omega$  – particle rotation velocity.

Let us consider to which degree conditions (5) are satisfied for the case of the motion of droplet suspension-carrying flow in channels, for instance, in a cylindrical pipe.

The first of these constraints indicates the necessity to observe a certain relationship between the sizes of the particles under consideration, the flow regime and the channel geometry. Indeed, with the use of the known ratios for the laminar sublayer, the considered constraint can be presented in the form of:

$$\sigma^2 \ll \frac{d^2}{4 \cdot 10^{-2} Re^{1.75}}, \tag{6}$$

where  $d$  is a pipe diameter,  $Re = \bar{U}_f d / \nu$ .

Table 1 shows the calculation results on (6) pertaining to correspondence with the required inequality, with the use of some arbitrarily chosen values of the parameters. It is clearly seen that constraint (6) is not significant for the most part of the range of these parameters and allows equation (4) to be used for them.

**Table 1 – Calculation results on inequality (6) correspondence**

Re	$d \cdot 10^3, m$	$\sigma \cdot 10^6, m$	$\sigma^2 \cdot 10^{12}, m$	$\frac{d^2}{4 \cdot 10^{-2} Re^{1.75}} \cdot 10^{12}, m$
$10^4$	20	1	1	$1 \cdot 10^3$
	50	2	4	$6.25 \cdot 10^3$
	200	5	25	$1 \cdot 10^5$
$5 \cdot 10^4$	20	1	1	$1.78 \cdot 10^2$
	50	2	4	$3.73 \cdot 10^2$
	200	5	25	$5.97 \cdot 10^2$
$10^5$	20	1	1	1.77
	50	2	4	$1.1 \cdot 10^2$
	200	5	25	$1.78 \cdot 10^3$

The presented data demonstrate only one exception, it concerns the regime of  $Re = 10^5$ ,  $d = 20$  mm,  $\sigma = 1.0 \mu m$ , at which the sets of parameters under comparison (given in columns 4 and 5 of Table 1) are comparable.

In the same way, it could be demonstrated that other constraints for (5) are also negligible from the point of view of possible use of Saffman's formula.

Taking all the foregoing into account, let us put down the particle motion equation within the laminar and part of the buffer (as quasi-laminar) layers for the vertically rising suspension-carrying flow in the circular pipe:

$$-6\pi\mu\sigma v_p - k\sigma^2(U_p - U_f) \sqrt{\mu\rho_f \left| \frac{dU_f}{dy} \right|} - \frac{1}{2} \left[ \frac{4}{3} \pi\sigma^3\rho_f \frac{dv_p}{d\tau} \right] = \frac{4}{3} \pi\sigma^3\rho_p \frac{dv_p}{d\tau}, \tag{7}$$

$$-6\pi\mu\sigma(U_p - U_f) - \frac{1}{2} \left[ \frac{4}{3} \pi\sigma^3\rho_f \left( \frac{dU_p}{d\tau} - \frac{dU_f}{d\tau} \right) \right] - \frac{4}{3} \pi\sigma^3(\rho_p - \rho_f)g = \frac{4}{3} \pi\sigma^3\rho_p \frac{dU_p}{d\tau}. \tag{8}$$

Equation (7) presents the balance of forces acting on the particle in the direction transverse to the main stream, i.e. along the Y-axis. In this case, the beginning of the Y-axis corresponds to the wall, and the direction towards the central line of the channel is assumed positive; so, the particle velocity in the course of its motion towards the wall will have a negative sign,  $v_p < 0$ .

Equation (8) presents the balance of forces acting on the particle in the X direction of the main stream (along the axis); with the upward direction of the axis assumed as positive.

The first terms in both equations are Stokes drag forces.

The second term in equation (7) stands for Saffman lift force, see equation (4), which at the rising flow is negative (directed towards the wall) only if  $U_p > U_f$ , i.e. at  $\rho_p < \rho_f$ , otherwise, its impact results in the opposite effect (from the wall).

The second term in equation (8) stands for the force that accelerates (moderates) the added mass of the particle relative to the flow. When gas flows were analyzed [4], this term was not introduced; however, in case of the dense particles motion in droplet flows, it should be taken into account.

The third term in equation (8) is a gravitation force; when  $\rho_p < \rho_f$ , it is a positive lift force. In case of the down flow, the plus sign should be in front of this term.

By solving the set of equations (7) and (8) for  $v_p$ , we get the second-order differential equation:

$$\frac{d^2v_p}{d\tau^2} + 2M \frac{dv_p}{d\tau} + (M^2 - N^2)v_p = D, \tag{9}$$

where

$$M = \frac{9}{2} \frac{\mu}{\sigma^2(\rho_p + 0.5\rho_f)},$$

$$N = \left( \frac{3k\mu\rho_p}{4\pi\sigma} \right)^{1/2} \frac{(dU_f/dy)^{3/4}}{v^{1/4}(\rho_p + 0.5\rho_f)},$$

$$D = \frac{3/4\pi(\rho_p - \rho_f)gk\mu(dU_f/dy)^{1/2}}{\rho_p^2\sigma v^{1/2}}.$$

After integration of differential equation (9), we get the solution of ( $M \neq N$ ) for the rising flow:

$$v_p = C_1 \exp(-M + N)\tau + C_2 \exp(-M - N)\tau + C_3, \quad (10)$$

And for the down flow:

$$v_p = C_1 \exp(-M + N)\tau + C_2 \exp(-M - N)\tau - C_3. \quad (11)$$

Constants  $C_1$  and  $C_2$  are determined from the initial conditions with the radial and axial velocity of the particle at the edge of the laminar sublayer, proceeding from the following assumptions [17]:

$$v_p^0(\tau = 0) = \sqrt{\overline{v_p'^2}} \Big|_{y=b} \approx 0.1\overline{U_f} \quad (12)$$

and 
$$U_p^0(\tau = 0) = \sqrt{\overline{U_p'^2}} \Big|_{y=b} \approx 0.2\overline{U_f}, \quad (13)$$

where  $v_p'$  and  $U_p'$  are radial and axial particle velocity fluctuations at the external boundary of the laminar sublayer; they are calculated from the respective root-mean-square velocity fluctuations of the carrying flow,  $v_f'$  and  $U_f'$ ;  $b$  is the laminar sublayer thickness. According to Laufer's data [5],  $v_f' = 0.1\overline{U_f}$ , and  $U_f' \approx 0.2\overline{U_f}$  (for  $Re = 10^4-10^5$ ), with all these things taken into account in equations (12) and (13).

Constant  $C_3$  was determined from the particular solution of equation (9) and is equal to:

$$C_3 = \frac{D}{M^2 - N^2} = \frac{(\rho_p - \rho_f)g(dU_f / dy)^{1/2}}{\frac{27\pi\mu v^{1/2}}{\sigma^3 k} - \rho_p(dU_f / dy)^{3/2}} = v_{pg}, \quad (14)$$

where  $v_{pg}$  is a radial (transverse) component of the particle velocity, which is not, as it can be seen, the function of time.

Thus, the solution of (10) and (11) can be presented as:

$$v_p = C_1 \exp(-M + N)\tau + C_2 \exp(-M - N)\tau \pm v_{pg}, \quad (15)$$

where the symbol (+) in front of the third addend is used at the rising flow, and the symbol (-) is used in case of the down flow.

With the use of equations (12) and (13), we get the set of equations for  $C_1$  and  $C_2$ , and with solving it we have:

$$C_1 = 0.5(v_p^0 - v_{pg}) - E, \quad (16)$$

$$C_2 = 0.5(v_p^0 - v_{pg}) + E, \quad (17)$$

where 
$$E = \frac{M \cdot v_{pg}}{2N} - \frac{21(\rho_p - \rho_f)g\sigma \sqrt{\frac{dU_f}{dy}}}{(\rho_p + 0.5\rho_f)N\sqrt{v}}. \quad (18)$$

**RESULTS**

In compliance with the solution of equation (15) and with consideration of (16)-(18), the required computer calculations were performed for the Pb-Bi ( $\rho_p < \rho_f$ ), Li ( $\rho_p > \rho_f$ ), and air ( $\rho_p \gg \rho_f$ ) flows in circular pipes. For the Pb-Bi alloy and Li it turned out that  $M \gg N$ , and for the air  $M < N$ . Besides, it is always the case that  $v_p^0 \gg v_{pg}$ , even if it is assumed that  $v_p^0 = 0,01 \bar{U}_f$ , see equation (12) to compare. Thus, for the Pb-Bi alloy and Li we have:

$$v_p = v_p^0 \exp(-M\tau) \pm v_{pg} \tag{19}$$

The path covered by the particle moving in the radial direction (with the velocity according to (19)), is equal to

$$S = \int_0^\tau v_p^0 \exp(-M\tau) d\tau \pm v_{pg} \cdot \tau \tag{20}$$

For the suspension-carrying droplet flows, sub-exponential factor  $M$  is high enough to assume without big errors that the upper limit of integration is equal to  $\tau = \infty$  (integral (20) quickly converges). Then:

$$S = \frac{v_p^0}{M} \pm v_{pg} \cdot \tau \tag{21}$$

At the same time, due to its only inertial motion the particle penetrates into the laminar sublayer to the depth of:

$$S' = \frac{v_p^0}{M} \tag{22}$$

As the calculation shows, this value only covers some fractions to a percent of the total thickness of the laminar sublayer, both for the lead-bismuth alloy and for lithium ( $M$  is close to the value of  $\beta$  used earlier in (3), when we considered only Stokes' drag force). Thus, the determining role in penetration of the particle deep into the laminar sublayer is played by the second terms of equations (19) and (21), so, we can put down that:

$$v_p = \pm v_{pg} \tag{23}$$

$$S = \pm v_{pg} \tau \tag{24}$$

Coming back to consideration of equation (14) for velocity  $v_{pg}$ , we can conclude that its physical significance consists in the impact on it of the acting gravitation effect ( $\rho_p \neq \rho_f$ ) that determines the appearance of transverse particle migration. However, it is distinctive that earlier, when suspension-carrying gas flows were considered [4], that effect was not detected.

For the rising motion  $v_p = v_{pg}$ . As for Pb-Bi  $\rho_p < \rho_f$  and  $v_{pg} > 0$ , following the calculation, there should be a slow drift of the particle towards the wall with a constant velocity. In the similar conditions for lithium ( $\rho_p > \rho_f$  and  $v_{pg} > 0$ ), the particle should migrate to the center of the flow [18-19].

For the downward motion, the situation changes to the opposite: as  $v_p = -v_{pg}$ , for the case of Pb-Bi the particle goes to the center of the flow, and for the case of Li it goes to the wall.

The analysis of calculated results for air has shown that in this case, when  $M < N$ , the radial velocity of the particle is actually influenced only by the first term in the right-hand part of equation (15), i.e.

$$v_p = C_1 \exp(-M + N)\tau \tag{25}$$

If  $C_1 < 0$  and  $M < N$ , there should be accelerated motion of a dense particle towards the wall, i.e. a completely different situation as compared to liquid. This fact is in agreement with the results of work [4], obtained numerically. At that, the effect of  $v_{pg}$  is weak as compared to that of the exponential term that has a positive index, equation (25).

Calculations for suspension-carrying flows were performed for the following range of the main parameters:

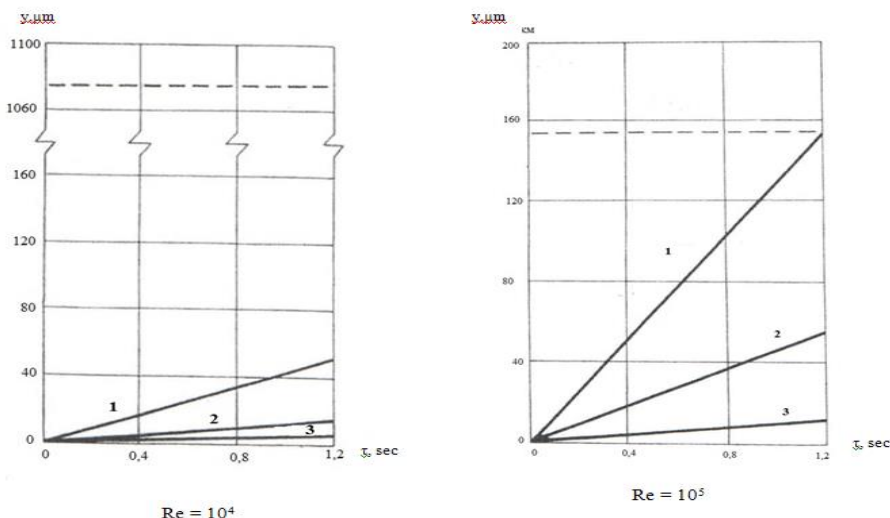
- Reynolds number  $Re = 10^4 - 10^5$ ;
- pipe diameter  $d = 5, 15, 45$  and  $135$  mm;
- particle radius  $\sigma = 1, 3, 5, 7$   $\mu\text{m}$ ;
- particle density  $\rho_p = 8 \text{ g/sm}^3, \rho_f = 10 \text{ g/sm}^3$  (Pb-Bi) and  $\rho_f = 0.5 \text{ g/sm}^3$  (Li);
- flow temperature  $t = 300^\circ\text{C}$  (Pb-Bi alloy, Li),  $t = 20^\circ\text{C}$  (air);
- Pb-Bi – rising motion, Li – downward motion.

The typical calculated results pertaining to the shape of trajectories of particles of various sizes in the laminar sublayer of the turbulent flows going upwards and downwards in the vertical pipe are plotted in Figure 2, for Pb-Bi (a) and Li (b), respectively. It can be seen that with the increase in the coolant velocity (Re number) and particle sizes it gets more probable that the particles will reach the wall (the dashed line indicates the laminar sublayer thickness). The comparison of these graphs for Pb-Bi and Li shows that probability of particles' reaching the wall for Li is higher; it can be evidently explained by the fact that Li has a higher value of the ratio  $\rho_p / \rho_f$ , as compared to the value of  $\rho_f / \rho_p$  for Pb-Bi. It should be stressed that the issue of whether the specific particle will reach the channel wall in the given conditions actually comes down to the questions of how long the particle is present in the laminar sublayer and how stable the geometrical characteristics of the channel are along the coolant flow.

Figure 3 illustrates the calculated acceleration of the solid particle motion to the wall with the air flow ( $t = 20^\circ\text{C}$ ) in the circular pipe,  $d = 30$  mm,  $Re = 10^4$ ,  $\sigma = 9$   $\mu\text{m}$ . In this case, the calculation shows that the initial velocity of the particle motion to the wall should be no less that the value calculated from the equation:

$$v_p^0 = v_{pg} + 2E, \tag{26}$$

where E comes from (18).



a) Pb-Bi



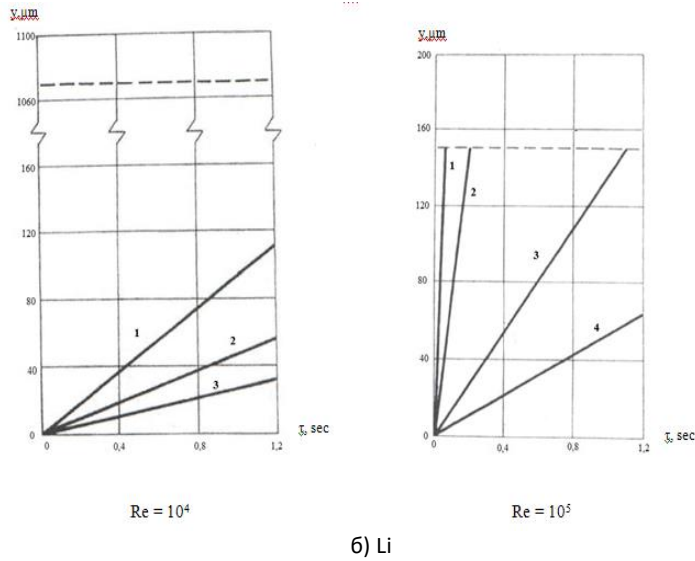


**Figure 2 – Kinetic motion trajectories of solid particles of various sizes towards the wall in the laminar sublayer of the Pb-Bi flow (a) going upwards and Li (b) downwards in the vertical pipe, d = 135 mm; particle diameter  $\sigma$ : 1) 7  $\mu\text{m}$ ; 2) 5  $\mu\text{m}$ ; 3) 3  $\mu\text{m}$ ; 4) 1  $\mu\text{m}$**

In order to confirm the obtained results of analytical calculations, the experiments were performed with the downward and upward motion of Pb-Bi coolant that contained suspended particles of a wide range of sizes resulted from corrosion-erosion processes in the circuit and oxygen ingress from the air. All in all, four pairs of working sections were tested in the same conditions to get the statistics, with each pair containing a section of upward and downward flows of the coolant (Figure 4). And in two pairs the first along the coolant way were the sections with the coolant upward flow and in two – with its downward flow.

The working section design is given in Figure 5. The inner and outer tubes form an annular gap through which, likewise through the central cylindrical part, the coolant circulates with a controlled flow rate measured by electromagnetic flow meters. The outer surface of the inner tubes was under control, by its condition it was possible to judge about the deposits formed as a result of transverse migration of particles from the annular gap to the wall.

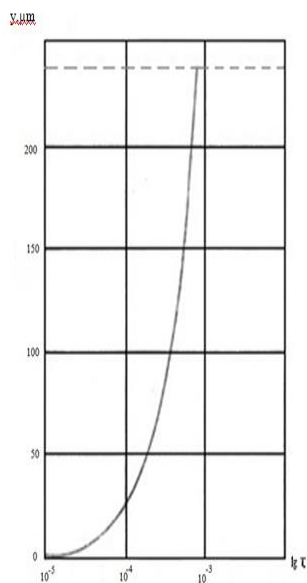


**Figure 3 – Particle motion in the viscous sublayer of air ( $t = 20\text{ }^{\circ}\text{C}$ ) in the circular pipe,  $d = 30\text{ mm}$ ,  $Re = 10^4$ ,  $\sigma = 9\text{ }\mu\text{m}$**

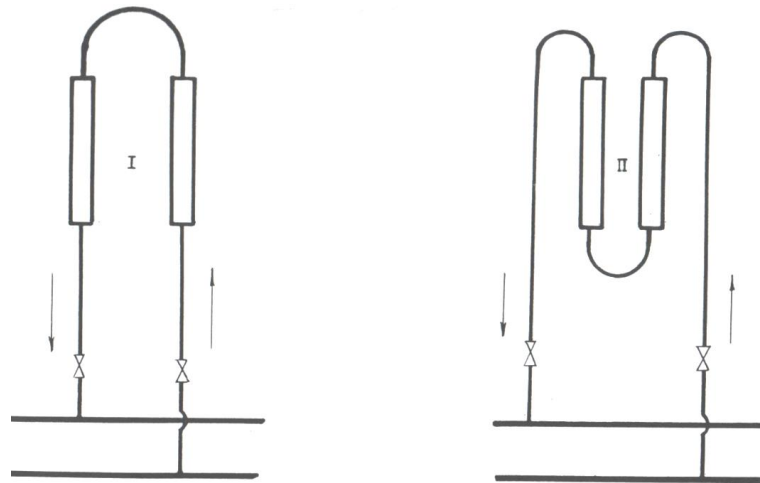


**Figure 4 – Layout of embedded working sections**  
I – sections 1-6; II – sections 7-8

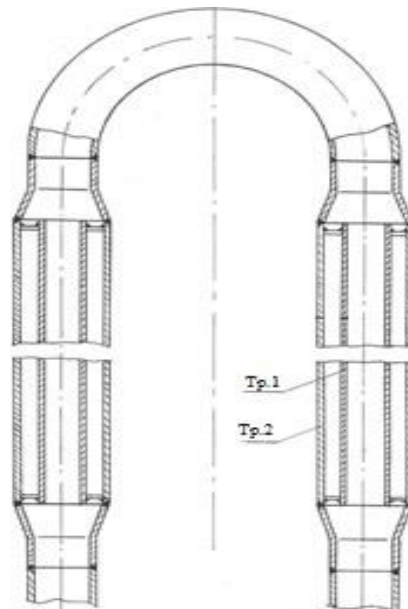


**Figure 5 – Working section design**

The data on the diameters of the working sections and respective materials they were fabricated of, as well as the main test characteristics are given in Table 2.

**Table 2 – Specifications of test working sections and test conditions**

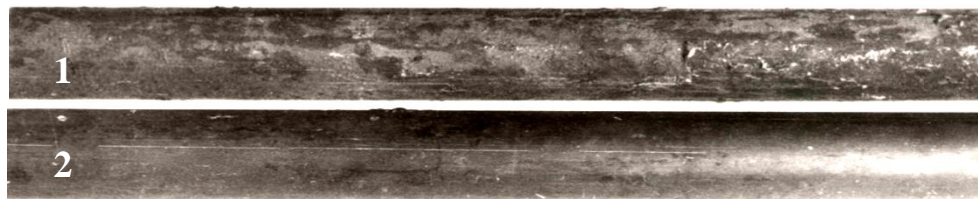
Section №	Material of the tube under control (Tp.1)	Tube 1, mm	Tube 2, mm	Test duration, h	Re number in annular gap
1	steel Cr18Ni10Ti (d)	45x3	57x4	200	$3,5 \cdot 10^3 - 7 \cdot 10^3$
2	steel Cr18Ni10Ti (r)	25x3	45x3		$1,55 \cdot 10^4 - 3,1 \cdot 10^4$
3	steel Cr18Ni10Ti (d)	25x3	45x3	250	$1,55 \cdot 10^4 - 3,1 \cdot 10^4$
4	steel EP-79 (r)	12x2	32x2.5		$3,3 \cdot 10^4 - 6,6 \cdot 10^4$
5	steel Cr18Ni10Ti (d)	25x3	45x3	250	$1,55 \cdot 10^4 - 3,1 \cdot 10^4$
6	steel Cr18Ni10Ti (r)	25x3	45x3		$1,55 \cdot 10^4 - 3,1 \cdot 10^4$
7	steel EP-79 (d)	12x2	32x2.5	300	$3,3 \cdot 10^4 - 6,6 \cdot 10^4$
8	steel EP-79 (r)	12x2	32x2.5		$3,3 \cdot 10^4 - 6,6 \cdot 10^4$

(d) –downcomer, (r) – riser

During the liquid metal circuit operation period preceding the experiments the coolant was accumulating suspended impurities (primarily, based on iron, chromium, lead and bismuth oxides) with a wide range of sizes. The coolant temperature was maintained at the level of 280-300 °C during the entire period of testing.

When the experiments for each pair of working sections were over, the coolant was drained and the circuit was cooled, the working sections were removed for the following study of the working surface states.

Figure 6 shows the photos for the comparative analysis of the outer surface states for the inner tubes of the downcomer and the riser under the influence of the Pb-Bi flow. For all the four pairs of the working sections tested a common tendency was clearly seen, namely: the deposits (with a thickness up to 100 μm) were observed on the risers, whereas on the downcomers there were actually no deposits. The same situation was typical of the inner surfaces of the outer tubes.



1 – riser, 2 – downcomer

Figure 6 – Photos of the surfaces of the inner tubes after tests in the circulating Pb-Bi

It was also found out that the inlet regions of the channels (with the distance up to 40-60 d) were usually free of deposits; it obviously confirms the role of the kinetic conditions required for the particle to reach the wall in the course of its migration through the laminar sublayer.

The X-ray crystal structure analysis of the deposits has shown that solid particles primarily of lead oxide (PbO) and such oxides as Fe<sub>3</sub>O<sub>4</sub> and Cr<sub>2</sub>O<sub>3</sub> represent the main slag-forming phase, with their total mass contents in the deposit usually not exceeding 5-8 mass % (the other part consists of the main coolant components, Pb and Bi). According to the data obtained with the electronic microscope, the particle sizes in the deposit were basically equal to 5-20 μm.

### CONCLUSION

The results of analytical calculations confirm the impact of the gravitation effect of the particles in the laminar sublayer of the turbulent suspension-carrying flow on the near-wall transverse migration of these particles; this fact quantitatively agrees with the obtained experimental data. It is demonstrated that in the dropping liquid the particle motion towards the wall or from it depends on the particle-liquid density ratio and the flow direction in the vertical channel: at  $\rho_p/\rho_f < 1$  the particle migration to the wall occurs at the rising flow, and at  $\rho_p/\rho_f > 1$  – with the down flow. At that, the transverse Saffman lift force effect increases when the flow velocity (Reynolds numbers) goes up and particle sizes grow. This fact should be taken into account, in particular, for prediction of possible deposits formation on the walls of vertical channels as the process system elements with suspension-carrying liquid and gas flows.

### GRATITUDE

The work was performed under Agreement No. 14.625.21.0001 of 21.08.2014 between the Ministry of Education and Science of Russian Federation and the JSC “SSC RF-IPPE” (the unique identifier of the project is RFMEF162514X0001).

### REFERENCES

- [1] Nigmatullin R. I. Dynamics of multiphase media. Vol. 1, Moscow, Nauka, 1987, p. 464.
- [2] Papyrin A.N. et al. Cold spray technology, UK. : Elsevier, 2007, 336p.

- [3] A.M. Posazhennikov, A. G. Grishin, I. V. Yagodkin, V. P. Melnikov. Development of the Electro-physical Method of Aero-ion Cleaning of Gaseous Atmosphere //J. Nuclear Physics and Engineering, 2015, Vol. 4, № 4, p. 349-354.
- [4] Dandy D.S., Dwyer H.A. A sphere in shear flow at finite Reynolds number: effect on partial lift, drag and heat transfer //J. Fluid Mech. 1990. V.216. P. 381-410.
- [5] Saffman P.G. The lift on small sphere in a slow shear flow// J. Fluid Mech. 1965. V.22. P.385-400. Corrigendum: //J. Fluid Mech. 1968. V.31. P.624.
- [6] Rubinow S.I., Keller J.B. The transverse force on a spinning sphere moving in a viscous fluid //J. Fluid Mech, 1961, 11. P.447-459
- [7] Yatsenko V. P. Determination of the force acting on a spherical solid particle in a flow with a shift of//, D. SC, 2002, №39, p. 240-248
- [8] Yatsenko V. P., Aleksandrov, V. V. Measurement of the Magnus force at moderate Reynolds numbers// journal of Applied fluid mechanics, 2001, vol. 3 (75), № 3, p. 83-87
- [9] Asmolov E. S. Transverse migration of small spherical particles in unsteady shear flows. Thesis for the degree of doctor of Phys-Math. of Sciences, Moscow state University, Moscow, 2005
- [10] Rybdylova O. D. Lateral migration and focusing of inertial particles in shear flows. Thesis for the candidate of Phys-Math. of Sciences, Moscow state University, Moscow, 2012
- [11] Mullary V. A. Influence of lateral forces on the distribution of particles in the flow of gas suspension in a pipe// Vestnik SPbGU ser.1 1996, vol. 3, No. 15, pp. 82-88
- [12] Rouhinen P.O. Stachiewisz J.M. American Society Mechanics Engineering/ 1969, NHT-41. P.11.
- [13] Osiptsov A.N. Mathematical modeling of dusty-gas boundary layers// Appl.Mech.Rev. 1997. V.50, № 6, p.357-370
- [14] Aoki H., Kurosaki Y., Anzai H. Study on the tubular pinch effect in a pipe flow// Bull. JSME. 1979.22.164. p. 206- 212
- [15] Jeffery R.G., Pearson J.R. Particle motion in laminar vertical tube flow// J. Fluid Mech. 1965, p. 721-735
- [16] Segre G., Silberberg A., Behaviour of macroscopic rigid spheres in Poiseuille flow, Pt.2 Experimental results and interpretation// J. Fluid Mech. 1962, V.14. p. 136-157
- [17] Townsend A. A., Structure of turbulent flow with transverse shift. Moscow, 1959.
- [18] Han M., Kim C., Kim N., Lee S. Particle migration in tube flow of suspensions// J. Rhed. 1999. 43. p. 1157-1174
- [19] Lee S.L. Aspects of suspension shear flow //Adv. in Appl. Mech., 1982, V. 22, P.1-65